Charalambos C. Baniotopoulos; Jaroslav Haslinger; Zuzana Morávková

Mathematical modeling of delamination and nonmonotone friction problems by hemivariational inequalities

Applications of Mathematics, Vol. 50 (2005), No. 1, 1–25

Persistent URL: http://dml.cz/dmlcz/134587

MATHEMATICAL MODELING OF DELAMINATION AND NONMONOTONE FRICTION PROBLEMS BY HEMIVARIATIONAL INEQUALITIES*

Charalambos C. Baniotopoulos, Thessaloniki, Jaroslav Haslinger, Praha, and Zuzana Morávková, Ostrava

(Received October 16, 2002, in revised version April 18, 2003)

Abstract. The paper deals with approximations and the numerical realization of a class of hemivariational inequalities used for modeling of delamination and nonmonotone friction problems. Assumptions guaranteeing convergence of discrete models are verified and numerical results of several model examples computed by a nonsmooth variant of Newton method are presented.

Keywords: approximation of hemivariational inequalities, delamination, nonmonotone friction

MSC 2000: 74G15, 74M10, 74M15

0. Introduction

Mathematical models of many problems in solid mechanics are given by an inclusion type problem:

$$(1.1)\qquad \begin{cases} \text{Find } u \in V \text{ such that} \\ f - Au \in Bu, \end{cases}$$

where V is an appropriate function space, $f \in V'$ (= dual of V), $A\colon V \mapsto V'$ is a *linear single valued* mapping and $B\colon V \mapsto V'$ is generally a *multivalued mapping*. When B is maximal monotone, problem (1.1) leads to a classical variational

* The research was realized in the frame of the bilateral cooperation between Charles University, Prague and Aristotle University, Thessaloniki. The second author also acknowledges the support of the grant no. IAA1075402 of the Grant Agency of the Academy of Sciences of the Czech Republic and MSM 113200007.

inequality, i.e. to the case which is now very well analysed from the theoretical as well as the computational point of view. The monotonicity assumption is however very restrictive. In practice we meet a lot of problems in which basic constitutive laws are no longer monotone and consequently more complicated models have to be used. *Hemivariational inequalities* (HI) represent a possible tool enabling us to involve nonmonotone and multivalued relations into mathematical models. They were introduced by P. D. Panagiotopoulos in the eighties. By means of (HI), phenomena such as nonmonotone friction and unilateral conditions, nonmonotone material laws and nonmonotone interface laws among different structural elements can be taken into account. The present paper deals with the modeling and the numerical realization of delamination processes in layered materials and with Signorini type problems involving nonmonotone friction between a body and a rigid foundation.

The paper is organized as follows: in Section 1 we present motivations for the use of tools of nonsmooth analysis in solid mechanics. In Section 2 we introduce the abstract formulation of a class of *constrained hemivariational inequalities of elliptic type*. We show how to discretize them in order to get a discrete (HI) which can be solved by methods of nonsmooth optimization. In Section 3 we use constrained (HI) to formulate simple delamination and nonmonotone friction problems in 2D. Numerical results of model examples are presented in Section 4. These examples are computed by using a nonsmooth variant of the Newton method.

1. Some mechanical motivations for the nonmonotone laws in the case of delamination and friction

During the 60s, the manufacture of advanced materials composed of laminated composites with high strength and resistance properties led to a rapid expansion of this modern branch of Material Science. During the last decades, a plethora of laminated composites emerging in the whole spectrum of technological applications with a huge significance in industry and in construction have been manufactured. It is noteworthy that the basic feature of laminated composites is that to the structures where they are used they give much better properties than their constituents do, thus leading to significantly increased safety, lower operation/preservation costs and ameliorated serviceability. Strength, stiffness, weight, fracture toughness, corrosion resistance, endurance and growth of crack resistance, thermal conductivity and interlaminar cohesion are, for instance, properties that can be appropriately predicted during the manufacturing process, for laminated composites with improved behavior with respect to the aforementioned properties to be obtained. This is the reason why laminated composites are nowadays applied to a wide range of structures in advanced technology applications.

Due to the great significance of laminated products in modern industry, the study of the mechanical response of laminated structures has during the last two decades attracted the interest of a plethora of researchers. The difficulty arising in connection with this investigation is due to the much more complicated behavior of laminated composites in comparison to that of their constituents. As a matter of fact, the phenomenon mainly dominating their structural performance is the interface delamination phenomenon combined with complex friction states. The latter effects can be described in a macroscopic way by means of nonmonotone, possibly multivalued stress-strain or reaction-displacement laws describing the delamination along the interlaminar phase in the presence of complex friction effects.

In the present study, an efficient numerical method is applied to quantify the toughness of laminated products under cleavage loading, taking into account delamination and nonmonotone friction effects between interply layers. Such a mechanical behavior can be described by nonmonotone, possibly multivalued stress-strain or force-displacement diagrams corresponding to laws that include complete jumps or decreasing branches; the latter simulate the abrupt reduction of the strength of laminates as soon as the critical value of stress or strain has been reached. These laws that are defined along the whole length of the strain or displacement axis and are derived by experimental tests, are called complete stress-strain or force-displacement diagrams. As a matter of fact, complete stress-strain or force-displacement diagrams in laminated composites exhibiting such softening behavior have been recently obtained by the use of advanced testing machines that minimize the range of destabilizing effects during the experimental procedure. A lot of nonmonotone experimental delamination and friction diagrams have been recently obtained during the testing of laminated specimens. For instance, the serrated force-displacement diagrams of Fig. 1.1a have been recently obtained from tests of fiber reinforced or unreinforced specimens of laminated products [3]. These diagrams define the brittle delamination initiation along the interfaces, as well as information on whether delamination is progressive or abrupt. Diagrams with similar features (cf. e.g. Fig. 1.1b) have been obtained during glass fiber-reinforced epoxy laminated specimens [11]. In the analysis of structural laminates, continuous friction stress redistribution occurs simultaneously with the successive delamination of plies until total delamination (Fig. 1.1e) [13]. Extensive testing programs carried out in order to evaluate the effect of the matrix resin on the impact delamination tolerance of graphite/epoxy composite laminates, led to a family of complete load-deflection curves (cf. e.g. the curve in Fig. 1.1d) where the descending branch corresponds to the nonmonotone friction effects after the initiation of delamination [14]. Similar diagrams have been obtained during the testing of clad metals (cf. e.g. the load-deflection curves illustrating the discontinuous response of beryllium/aluminium composite laminates during a three-point test

(Fig. 1.1e)) [12]. The well-known Scanlon's diagram for the tension stiffening effect of reinforced concrete (Fig. 1.1f) is also similar to a lot of experimental diagrams obtained for laminated composites [8].

As a matter of fact, in all the previous cases, as soon as delamination between the laminated plies starts, friction forces also start playing a dominant role in the mechanical behavior of the laminated structure. The friction diagram that describes these effects is not any more a classic Coulomb type one, but a generalized curve with decreasing and re-increasing branches; this nonmonotone curve is derived by a nonconvex friction law [10], [7].

The analysis of the delamination problem with nonconvex friction effects within the variational methods framework and the effort to incorporate the respective results into an effective finite element model are in detail presented in the next sections.

2. Constrained hemivariational inequalities and their approximation

The aim of this section is to give the abstract setting of a large class of constrained hemivariational inequalities of elliptic type and to describe its approximation. We start with notation.

Let $\Omega \subset \mathbb{R}^2$ be a bounded domain with a Lipschitz boundary $\partial\Omega$, let $V \subset (H^1(\Omega))^2$ be a subspace, $\| \, \|$ the norm in V, and $K \subseteq V$ a non-empty, closed, convex subset of V. Here we restrict ourselves to the plane case. If $\Omega \subset \mathbb{R}^n$, $n \geqslant 3$, the existence result for $(\mathcal{P})$ remains true but its discretization, in particular the definition of the finite element spaces, has to be modified.

We denote by $a\colon V \times V \mapsto \mathbb{R}$ a bilinear form which is bounded and V-elliptic in V. Further, let Z be a space of real-valued functions defined in a measurable set $\omega \subseteq \partial\Omega$ and let $\Pi\colon V \mapsto Z$ be a linear mapping. Finally, let Y be another space of real functions defined in ω being in duality with Z. The respective duality between Z and Y will be denoted by $\langle \, , \, \rangle_{Y\times Z}$ while $\langle \, , \, \rangle$ stands for the duality pairing between V and V'.

By a solution of the *constrained hemivariational inequality* defined by the above data we mean a pair $(u, \Xi) \in K \times Y$ satisfying

$$(\mathcal{P}) \qquad \begin{cases} a(u, v-u) + \langle \Xi, \Pi v - \Pi u \rangle_{Y\times Z} \geqslant \langle f, v-u \rangle \quad \forall\, v \in K \\ \Xi(x) \in \hat{b}(\Pi u(x)) \quad \text{for a.a. } x \in \omega, \end{cases}$$

where $f \in V'$ is a given element and $\hat{b}\colon \mathbb{R} \to 2^{\mathbb{R}}$ is a multifunction whose construction will be now described.

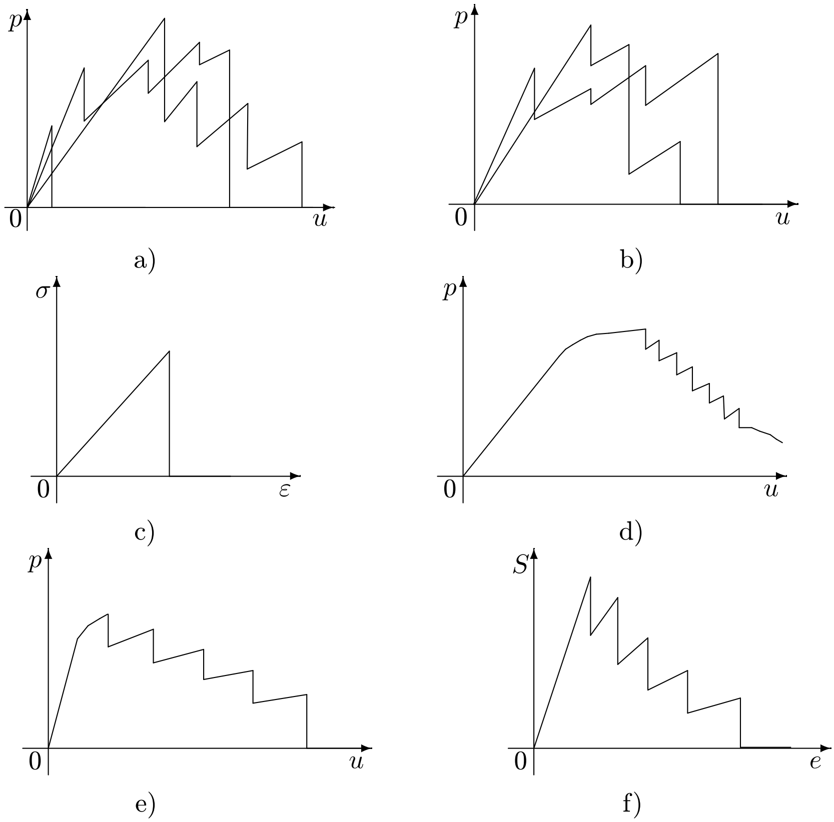

Figure 1.1. a) Force-displacement diagrams for laminated products
b) Force-displacement diagrams for glass fiber-reinforced epoxy laminated composites
c) Ply stress-strain curve in a lamina with brittle behavior
d) Force-displacement diagram for a graphite-epoxy composite laminate
e) Force-displacement diagram for an aluminium-beryllium composite beam
f) Scanlon's diagram

Let $b \in L^{\infty}_{\mathrm{loc}}(\mathbb{R})$ be a locally bounded and measurable function satisfying the following sign condition:

$$\exists\,\overline{\xi} > 0 \quad \text{such that} \quad \operatorname*{ess\,sup}_{\xi \in (-\infty, -\overline{\xi})} b(\xi) \leqslant 0 \leqslant \operatorname*{ess\,inf}_{\xi \in (\overline{\xi}, \infty)} b(\xi). \tag{2.1}$$

For every $\varepsilon > 0$ we define two auxiliary functions $\underline{b}_\varepsilon, \overline{b}_\varepsilon \colon \mathbb{R} \mapsto \mathbb{R}$ by

$$\underline{b}_\varepsilon(\xi) = \operatorname*{ess\,inf}_{|\tau - \xi| \leqslant \varepsilon} b(\tau), \quad \overline{b}_\varepsilon(\xi) = \operatorname*{ess\,sup}_{|\tau - \xi| \leqslant \varepsilon} b(\tau).$$

The limits of $\underline{b}_\varepsilon$ and $\overline{b}_\varepsilon$ for $\varepsilon \to 0+$ will be denoted by $\underline{b}$ and $\overline{b}$, respectively. The functions $\underline{b}$ and $\overline{b}$ define the following multifunction $\hat{b}\colon \mathbb{R} \to 2^{\mathbb{R}}$:

$$\hat{b}(\xi) = [\underline{b}(\xi), \overline{b}(\xi)] \quad \forall\, \xi \in \mathbb{R},$$

i.e. $\hat{b}$ results from the generally discontinuous function b by filling in the gaps at the points of its discontinuity. Observe that we do not require any monotonicity of b meaning that $\hat{b}$ may involve also *decreasing* branches.

In our particular problems studied in this paper we will suppose that the function b satisfies an additional growth condition, namely

$$|b(\xi)| \leqslant c_1 + c_2|\xi|^{q/q'} \quad \text{for a.a. } \xi \in \mathbb{R}, \tag{2.2}$$

where c_1, c_2 are positive constants and $1/q + 1/q' = 1$ with $q \in (1, \infty)$. Further we will suppose that the linear mapping Π is continuous from V into $L^q(\omega)$:

$$\exists\, c = \text{const} > 0\colon\ \|\Pi v\|_{L^q(\omega)} \leqslant c\|v\| \ \ \forall\, v \in V. \tag{2.3}$$

If it is so one can specify the spaces Y and Z appearing in the definition of $(\mathcal{P})$ as follows: $Y = L^{q'}(\omega)$, $Z = L^q(\omega)$ and the duality pairing between Y and Z is realized by the integral over ω.

If (2.1)–(2.3) are satisfied then the constrained hemivariational inequality $(\mathcal{P})$ has a solution $(u, \Xi) \in K \times L^{q'}(\omega)$. The proof of this assertion can be done directly or by using the tools of multivalued analysis, or it follows from the convergence results established in [4] (see also Theorem 2.1 below).

R e m a r k 2.1. If the bilinear form a is *symmetric* then problem $(\mathcal{P})$ is related (but not equivalent, see [1] and Theorem 2.2 below for the discrete case) to the following *substationary* type problem:

$$\text{Find } u \in V\colon\ 0 \in \overline{\partial} L(u) + N_K(u), \tag{$(\mathcal{P})'$}$$

where

$$L(v) = \frac{1}{2}a(v, v) - \langle f, v\rangle + \Phi(v),$$
$$\Phi(v) = \int_\omega \int_0^{\Pi v} b(t)\,\mathrm{d}t\,\mathrm{d}s.$$

Here $N_K(u)$ is the normal cone of K at u and $\overline{\partial}$ denotes the generalized gradient in the sense of Clarke. Unlike classical linear elasticity problems, the total potential energy functional L is neither convex nor differentiable just due to the presence of the term Φ which is generally only a Lipschitz continuous function in V.

Next we briefly describe a possible discretization of $(\mathcal{P})$. For the sake of simplicity we will suppose that $\Omega \subset \mathbb{R}^2$ is a *polygonal* domain. Let $h > 0$ be a discretization parameter and let $\mathcal{D}_h, \mathcal{T}_h$ be a triangulation of $\overline{\Omega}$ and a partition of $\overline{\omega}$ into triangles T and segments S, respectively. With every $\mathcal{D}_h, \mathcal{T}_h$ the following finite dimensional spaces will be associated:

$$V_h = \{v_h \in (C(\overline{\Omega}))^2 \mid v_{h|T} \in (P_1(T))^2 \ \ \forall T \in \mathcal{D}_h\} \cap V,$$
$$Y_h = \{\mu_h \in L^\infty(\omega) \mid \mu_{h|_S} \in P_0(S) \ \ \forall S \in \mathcal{T}_h\},$$

i.e. V_h is the space of all continuous *piecewise linear* functions over $\mathcal{D}_h$ satisfying the same boundary conditions as the functions from V and Y_h is the space of all *piecewise constant* functions over $\mathcal{T}_h$. The spaces V_h, Y_h are discretizations of V, Y, respectively. Let $\{K_h\}$, $h \to 0+$, $K_h \subset V_h$, be a system of closed, convex subsets discretizing the set K. Observe that we do not require $K_h \subset K$, $\forall\, h > 0$. Finally, denote by $W_h \subset Z$ the image of V_h with respect to the mapping Π appearing in the definition of $(\mathcal{P})$:

$$W_h = \Pi(V_h) \quad \forall\, h > 0,$$

and introduce a linear mapping $P_h\colon W_h \mapsto Y_h$ (in the next section we shall specify a particular choice of P_h which will we used in our computations). In the interior of each segment $S_i \in \mathcal{T}_h$ we choose and fix just one point x^i_h. The values of functions from Y_h at x^i_h will be interpreted as the degrees of freedom. We are now ready to define the following *discrete hemivariational inequality*:

$$(\mathcal{P})_h \quad \begin{cases} \text{Find } \ (u_h, \Xi_h) \in K_h \times Y_h \ \text{ such that} \\ a(u_h, v_h - u_h) + \int_\omega \Xi_h P_h(\Pi v_h - \Pi u_h)\,\mathrm{d}s \geqslant \langle f, v_h - u_h\rangle \ \ \forall\, v_h \in K_h \\ \Xi_h(x^i_h) \in \hat{b}(P_h(\Pi u_h)(x^i_h)) \ \ \forall\, i. \end{cases}$$

R e m a r k 2.2. Problem $(\mathcal{P})_h$ is a standard Galerkin method: instead of K, Y we use appropriate finite dimensional discretizations K_h, Y_h. The role of the auxiliary mapping P_h in the definition of $(\mathcal{P})_h$ is to map functions from W_h into the space to which the second component Ξ_h belongs.

Convergence results, i.e. the analysis of a relation between solutions to $(\mathcal{P})$ and $(\mathcal{P})_h$ as $h \to 0+$ are established in [4].

Let us recall briefly the assumptions under which solutions to $(\mathcal{P})$ and $(\mathcal{P})_h$ are close on subsequences as $h \to 0+$. In addition to (2.1)–(2.3) we shall suppose:

$$(2.4) \qquad \begin{cases} \text{the mappings } \ P_h\colon W_h \mapsto Y_h, \ \ h \to 0+ \ \text{ satisfy} \\ y_h \rightharpoonup y \ \text{ (weakly) in } \ V, \quad y_h \in V_h \Rightarrow \exists\, s \geqslant q \ \text{ such that} \\ \|P_h(\Pi y_h) - \Pi y\|_{L^s(\omega)} \to 0 \ \text{ as } \ h \to 0+; \end{cases}$$

and

$$\text{the system } \{K_h\},\ h \to 0+ \ \text{ is such that}$$

$$0 \in K_h \ \ \forall\, h; \tag{2.5}$$

$$\forall\, v \in K \ \ \exists\, \{v_h\},\ \ v_h \in K_h\colon\ v_h \to v \ \text{ in } \ V,\ \ h \to 0+; \tag{2.6}$$

$$v_h \rightharpoonup v \ \text{ in } \ V,\ \ v_h \in K_h \Rightarrow v \in K. \tag{2.7}$$

If (2.1)–(2.3) are satisfied then there exists *at least* one solution (u_h, Ξ_h) of $(\mathcal{P})_h$ for every $h > 0$ and, in addition, there is a positive constant c such that

$$\|u_h\| \leqslant c, \quad \|\Xi_h\|_{L^{q'}(\omega)} \leqslant c \quad \forall\, h > 0$$

(see Lemma 3.8 and Theorem 3.8 in [4]).

The main convergence result is formulated in the next theorem.

Theorem 2.1. *Let* (2.1)–(2.7) *be satisfied. Further let* $\{(u_h, \Xi_h)\}$ *be a sequence of solutions to* $(\mathcal{P})_h$*,* $h > 0$ *with* $\{(u_h, \Xi_h)\}$ *being bounded. Then there exist a subsequence* $\{(u_{h'}, \Xi_{h'})\}$ *of* $\{(u_h, \Xi_h)\}$ *and a pair* $(u, \Xi) \in K \times L^{q'}(\omega)$ *such that*

$$\begin{cases} u_{h'} \to u & \text{in } V, \\ \Xi_{h'} \rightharpoonup \Xi & \text{in } L^{q'}(\omega), \ \text{ as } h' \to 0+ \end{cases} \tag{2.8}$$

where the number q' *is from* (2.2)*. The pair* (u, Ξ) *solves* $(\mathcal{P})$*. Furthermore, any cluster point of* $\{(u_h, \Xi_h)\}$ *in the sense of* (2.8) *solves* $(\mathcal{P})$*.*

As we have already mentioned, the solution (u_h, Ξ_h) to $(\mathcal{P})_h$ is not unique, in general. Let us suppose that the first component u_h is already known. A natural question arises, namely, under which condition the knowledge of u_h determines Ξ_h in a unique way, i.e. if (u_h, Ξ_h), $(u_h, \overline{\Xi}_h)$ are two solutions of $(\mathcal{P})_h$ with the same first component u_h when $\Xi_h = \overline{\Xi}_h$? Suppose that $K_h = V_h$. Then it is very easy to show (see Theorem 3.2. in [4]) that this property holds provided

$$P_h \ \text{ maps } \ W_h \ \text{ onto } \ Y_h. \tag{2.9}$$

Even if $K_h \subsetneqq V_h$ one can obtain Ξ_h from the knowledge of u_h (see [4, Section 3.6]).

To have a better idea of the problem we solve let us present the algebraic formulation of $(\mathcal{P})_h$ for $h > 0$ fixed.

Let $\dim V_h = n$, $\dim W_h = p$ and $\dim Y_h = m$. Then V_h, W_h and Y_h can be identified with $\mathbb{R}^n$, $\mathbb{R}^p$ and $\mathbb{R}^m$, respectively, and K_h with a closed convex subset $\mathcal{K} \subset \mathbb{R}^n$.

Further, let $\mathbf{\Pi}$ and $\boldsymbol{P}$ be $(p \times n)$, $(m \times p)$ matrices, representing the mappings $\Pi_{|V_h}$ and P_h, respectively. Since the function behind the integral over ω is piecewise constant, the respective integral can be evaluated exactly. Indeed,

$$\int_\omega \Xi_h P_h(\Pi v_h)\,\mathrm{d}s = \sum_{i=1}^m c_i \Xi_i (\boldsymbol{P}(\mathbf{\Pi}\boldsymbol{v}))_i,$$

where $\mathbf{\Xi} = (\Xi_1, \ldots, \Xi_m)$ is the vector representing $\Xi_h \in Y_h$ and $c_i = \operatorname{meas} S_i$, $S_i \in \mathcal{T}_h$. Setting $\Xi_i := c_i \Xi_i$ we can write $(\mathcal{P})_h$ in the following algebraic form:

$$(\vec{\mathcal{P}}) \qquad \begin{cases} \text{Find } (\boldsymbol{u}, \mathbf{\Xi}) \in \mathcal{K} \times \mathbb{R}^m \text{ such that} \\ (\boldsymbol{A}\boldsymbol{u}, \boldsymbol{v} - \boldsymbol{u})_{\mathbb{R}^n} + (\mathbf{\Xi}, \mathbf{\Lambda}(\boldsymbol{v} - \boldsymbol{u}))_{\mathbb{R}^n} \geqslant (\boldsymbol{f}, \boldsymbol{v} - \boldsymbol{u})_{\mathbb{R}^n} \ \forall \boldsymbol{v} \in \mathcal{K} \\ \Xi_i \in c_i \hat{b}((\mathbf{\Lambda}\boldsymbol{u})_i) \ \forall i = 1, \ldots, m \end{cases}$$

where $\boldsymbol{A}$ is the standard stiffness matrix, $\mathbf{\Lambda} := \boldsymbol{P}\mathbf{\Pi}$ is the $(m \times n)$ matrix, $(\ ,\ )_{\mathbb{R}^q}$ stands for the classical scalar product in $\mathbb{R}^q$, $\boldsymbol{f}$ is the discrete load vector and $\boldsymbol{u}$ is the vector of the nodal values of u_h. Problem $(\vec{\mathcal{P}})$ is termed the *constrained algebraic hemivariational inequality.*

Since we are not able to solve $(\vec{\mathcal{P}})$ directly we shall eliminate the second component $\mathbf{\Xi}$. Next we shall suppose that the bilinear form a is also *symmetric* implying the symmetry of $\boldsymbol{A}$. We shall proceed as in Remark 2.1. Let Φ_h be the locally Lipschitz functional on V_h defined by

$$\Phi_h(v_h) = \int_\omega \int_0^{P_h(\Pi v_h)} b(t)\,\mathrm{d}t\,\mathrm{d}s \quad v_h \in V_h.$$

We shall approximate Φ_h by applying the rectangular formula to the integral over ω:

$$\Phi_h(v_h) \approx \sum_{i=1}^m c_i \int_0^{P_h(\Pi v_h)(x_h^i)} b(t)\,\mathrm{d}t := \Psi(\boldsymbol{v}) \tag{2.10}$$

where $c_i = \operatorname{meas} S_i$, $S_i \in \mathcal{T}_h$ and $\{x_h^i\}$ are the same as in the definition of $(\mathcal{P})_h$. By $\mathcal{L}$ we denote the *discrete superpotential* corresponding to the algebraic (HI):

$$\mathcal{L}(\boldsymbol{v}) = \frac{1}{2}(\boldsymbol{A}\boldsymbol{v}, \boldsymbol{v})_{\mathbb{R}^n} - (\boldsymbol{f}, \boldsymbol{v})_{\mathbb{R}^n} + \Psi(\boldsymbol{v}), \quad \boldsymbol{v} \in \mathbb{R}^n. \tag{2.11}$$

Instead of $(\vec{\mathcal{P}})$ we shall consider the following *substationary type problem*:

$$(\vec{\mathcal{P}})' \qquad \begin{cases} \text{Find } \boldsymbol{u} \in \mathbb{R}^n \text{ such that} \\ \mathbf{0} \in \overline{\partial}\mathcal{L}(\boldsymbol{u}) + N_{\mathcal{K}}(\boldsymbol{u}), \end{cases}$$

where $\overline{\partial}$, $N_{\mathcal{K}}$ have the same meaning as in Remark 2.1.

Problems $(\vec{\mathcal{P}})$ and $(\vec{\mathcal{P}})'$ *are not* fully equivalent. Indeed, let $\boldsymbol{u} \in \mathcal{K}$ be a solution to $(\vec{\mathcal{P}})'$. Then there exists $\boldsymbol{\Xi} \in \mathbb{R}^m$ such that the pair $(\boldsymbol{u}, \boldsymbol{\Xi})$ solves $(\vec{\mathcal{P}})$. On the contrary, if $(\boldsymbol{u}, \boldsymbol{\Xi})$ is a solution to $(\vec{\mathcal{P}})$ then additional assumptions are needed in order to interpret $\boldsymbol{u}$ as a substationary point of $\mathcal{L}$. We have (see [4, p. 137]):

Theorem 2.2. *Let there exist one-sided limits $b(\xi\pm)$ for every $\xi \in \mathbb{R}$ and let* (2.9) *be satisfied. If $(\boldsymbol{u}, \boldsymbol{\Xi}) \in \mathcal{K} \times \mathbb{R}^m$ is a solution of $(\vec{\mathcal{P}})$ then $\boldsymbol{u}$ is a substationary point of $\mathcal{L}$ on $\mathcal{K}$ and $\boldsymbol{\Lambda}^T \boldsymbol{\Xi} \in \overline{\partial} \Psi(\boldsymbol{u})$.*

The reason why $(\vec{\mathcal{P}})$ is replaced by $(\vec{\mathcal{P}})'$ is that the latter can be solved by nonsmooth bundle type minimization methods. Having $\boldsymbol{u}$ at our disposal, we can recover also the vector $\boldsymbol{\Xi}$ such that the pair $(\boldsymbol{u}, \boldsymbol{\Xi})$ solves $(\vec{\mathcal{P}})$. In addition, if all the assumptions of Theorem 2.2 are satisfied then one can not miss (at least theoretically) some of the solutions to $(\vec{\mathcal{P}})$.

3. Formulation of delamination and nonmonotone friction problems by (HI) and their approximation

We start with the formulation of delamination problems. Let us consider a two-dimensional laminated structure shown in Fig. 3.1.

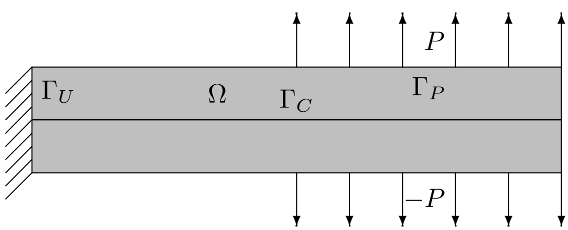

Figure 3.1.

Both layers are made of the same linear isotropic material obeying the plane stress model, characterized by the modulus of elasticity E, Poisson's ratio σ and the element thickness t. The structure is fixed along Γ_U, i.e. the zero displacements in both directions are prescribed:

$$u_i = 0 \text{ on } \Gamma_U, \quad i = 1, 2. \tag{3.1}$$

The upper and lower surface Γ_P of the lamina is subject to a perpendicular *opening* surface tractions $T = (0, \pm P)$, where $P \in L^2(\Gamma_P)$, $P \geqslant 0$ a.e. on Γ_P (see Fig. 3.1).

The volume forces are equal to zero. The interface behavior is described by a non-monotone multivalued function $\hat{b}$ which characterizes the bending interlayer material placed on Γ_C, more precisely the law between $-T_2(x)$ (the normal component of the stress vector) and the jump $[u_2(x)] := u_2^{(1)}(x) - u_2^{(2)}(x)$, where $u_2^{(1)}(x)$, $u_2^{(2)}(x)$ are the normal displacements of the upper and lower laminae, respectively, at $x \in \Gamma_C$. The interaction in the tangential direction will be neglected. Thus on Γ_C the following conditions are given:

$$\begin{cases} T_1(x) = 0, \quad x \in \Gamma_C \\ -T_2(x) \in \begin{cases} \hat{b}([u_2(x)]) & \text{if } [u_2(x)] > 0 \\ (-\infty, 0\rangle & \text{if } [u_2(x)] = 0, \quad x \in \Gamma_C. \end{cases} \end{cases} \tag{3.2}$$

In addition, the unilateral condition

$$[u_2] \geqslant 0 \quad \text{on } \Gamma_C \tag{3.3}$$

is prescribed. Due to the symmetry of the problem we may consider only the upper part of the structure. In this case the unilateral condition (3.3) becomes

$$u_2 \geqslant 0 \quad \text{on } \Gamma_C. \tag{3.4}$$

The boundary conditions (3.1)–(3.3) are completed by the system of equilibrium equations

$$\frac{\partial \tau_{ij}(u)}{\partial x_j} = 0 \quad \text{in } \Omega, \quad i = 1, 2, \tag{3.5}$$

where Ω is the rectangle representing the upper lamina and the stress tensor $\{\tau_{ij}(u)\}_{i,j=1}^2$ is related to the linearized strain tensor $\{\varepsilon_{ij}(u)\}_{i,j=1}^2$ by means of the linear Hooke's law

$$\tau_{ij}(u) = \frac{E\sigma}{1-\sigma^2}\delta_{ij}\vartheta + \frac{E}{1+\sigma}\varepsilon_{ij}(u), \quad i, j = 1, 2. \tag{3.6}$$

Here $\vartheta := \varepsilon_{ii}(u)$ is the trace of $\{\varepsilon_{ij}(u)\}_{i,j=1}^2$ and δ_{ij} is the Kronecker symbol.

By a *classical solution* of the delamination problem we mean a displacement field $u = (u_1, u_2)$ satisfying the boundary conditions (3.1)–(3.3) and the equations (3.5) with the linear Hooke's law (3.6). In order to give the weak formulation of the delamination problem we introduce the following notation:

$$\begin{aligned} V &= \{v \in (H^1(\Omega))^2 \mid v_i = 0 \quad \text{on } \Gamma_U,\ \ i = 1,2\}, \\ K &= \{v \in V \mid v_2 \geqslant 0 \quad \text{on } \Gamma_C\}, \\ a(u,v) &= \int_\Omega \tau_{ij}(u)\varepsilon_{ij}(v)\,\mathrm{d}x, \\ L(v) &= \int_{\Gamma_P} P v_2 \,\mathrm{d}x_1, \end{aligned}$$

where Γ_P is the upper surface of Ω subject to the tractions P.

The *weak formulation* of the delamination problem is given by the following hemivariational inequality:

$$(3.7) \qquad \begin{cases} \text{Find } (u,\Xi) \in K \times L^2(\Gamma_C) \text{ such that} \\ a(u, v-u) + \int_{\Gamma_C} \Xi(v_2 - u_2)\,\mathrm{d}x_1 \geqslant L(v-u) \quad \forall v \in K \\ \Xi(x) \in \hat{b}(2u_2(x)) \quad \text{for a.a. } x \in \Gamma_C \end{cases}$$

with the data introduced above (observe that $[u_2(x)] = 2u_2(x)$ due to symmetry). It is easy to see that $\Xi(x) = -T_2(x)$ if $u_2(x) > 0$ and $-T_2(x) \leqslant \Xi(x)$ if $u_2(x) = 0$.

A typical multivalued function $\hat{b}$ characterizing delamination problems is depicted in Fig. 3.2. Next we will suppose that the function b defining $\hat{b}$ satisfies the assumptions (2.1) and (2.2) with $q = q' = 2$.

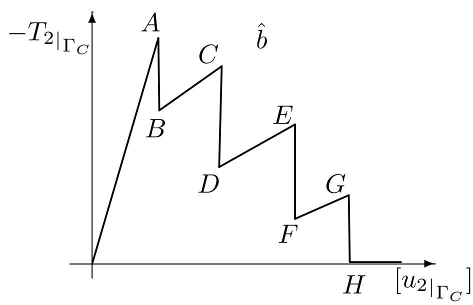

Figure 3.2.

We see that (3.7) results from the abstract formulation $(\mathcal{P})$ for the following data: $Y = L^2(\Gamma_C)$, $Z = L^2(\Gamma_C)$, $\omega = \Gamma_C$, $\Pi v = v_2$, where $v = (v_1, v_2) \in V$ and $\langle\,,\rangle_{Y\times Z}$ stands for the $L^2(\Gamma_C)$-scalar product. Since (2.2) and (2.3) are satisfied with $q = q' = 2$, the hemivariational inequality (3.7) has at least one solution in the indicated spaces.

Next we briefly describe the discretization of (3.7). Let $\{\mathcal{D}_h\}$, $h \to 0+$ be a system of *regular* triangulations of $\overline{\Omega}$. By V_h we denote the space of all continuous, piecewise linear vector functions on $\mathcal{D}_h$ vanishing on Γ_U. The closed convex set K is discretized by $K_h := V_h \cap K$.

It remains to construct the space Y_h. Let $x_h^{i+1/2}$ be the midpoint of the interval $[x_h^i, x_h^{i+1}]$, $i = 0, \dots, m-1$, where $\{x_h^i\}_{i=0}^m$ is the set of all nodes of $\mathcal{D}_h$ placed on $\overline{\Gamma}_C$. Next we shall suppose that $\{x_h^i\}_{i=0}^m$ forms an *equidistant* partition of Γ_C whose norm is h. The partition $\mathcal{T}_h$ of $\overline{\Gamma}_C$ defining the space Y_h consists of all segments S_i joining the midpoints $x_h^{i-1/2}$, $x_h^{i+1/2}$, $i = 2, \dots, m-1$ with the following modifications concerning S_1 and S_m (see Fig. 3.3):

$$S_1 = [x_h^0, x_h^{3/2}], \quad S_m = [x_h^{m-1/2}, x_h^m].$$

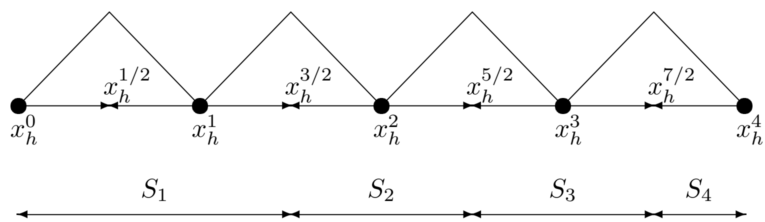

Figure 3.3.

On every $\mathcal{T}_h$ we will define the space Y_h of all piecewise constant functions with values at $\{x_h^i\}_{i=1}^m$ as the degrees of freedom. It is readily seen that in our particular case the space $W_h := \Pi V_h$ consists of all continuous piecewise linear scalar functions over the partition defined by the nodes $\{x_h^i\}_{i=0}^m$ and vanishing at the initial node x_h^0. Due to the definition of Y_h we also see that $\dim W_h = \dim Y_h$. It remains to specify the mapping $P_h \colon W_h \mapsto Y_h$ appearing in the definition of $(\mathcal{P})_h$. We use the following definition of P_h:

$$P_h(w_h) = \sum_{i=1}^m w_h(x_h^i) \chi_{S_i}(x_1), \quad w_h \in W_h,$$

where χ_{S_i} is the characteristic function of the interior of S_i. This mapping associates with a function $w_h \in W_h$ its piecewise constant Lagrange interpolate on $\mathcal{T}_h$ (see Fig. 3.4).

We are now able to define the following *discrete* (HI) approximating (3.7):

$$(3.8) \qquad \begin{cases} \text{Find } (u_h, \Xi_h) \in K_h \times Y_h \text{ such that} \\ a(u_h, v_h - u_h) + \int_{\Gamma_C} \Xi_h P_h(v_{h2} - u_{h2}) \,\mathrm{d}x_1 \geqslant L(v_h - u_h) \\ \quad \forall\, v_h = (v_{h1}, v_{h2}) \in K_h \\ \Xi_h(x_h^i) \in \hat{b}(2P_h(u_{h2})(x_h^i)) \quad \forall i = 1, \dots, m \end{cases}$$

with the data defined at the beginning of this section.

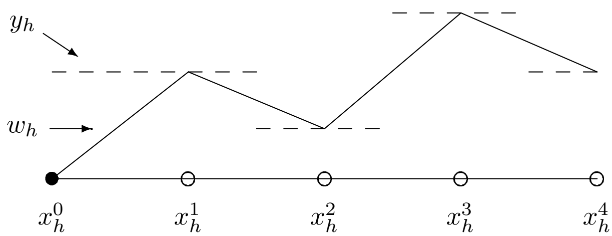

Figure 3.4.

Next we shall show that all assumptions of Theorem 2.1 are satisfied meaning that (3.8) approximates (3.7) in a sense specified below. The assumptions (2.1)–(2.3) are already fulfilled for the continuous setting of the problem. For this reason we confine ourselves to the verification of (2.4) and (2.6) ((2.7) is automatically satisfied since K_h is an internal approximation of K). The property (2.4) is satisfied with $s = q = 2$ as follows from [2]. It remains to verify (2.6). The proof is based on the following density result:

Lemma 3.1. *Let*

$$K_1 = \{v \in H^1(\Omega) \mid v = 0 \text{ on } \Gamma_U, \ \ v \geqslant 0 \text{ on } \Gamma_C\},$$

where $\Omega = (0, a) \times (0, b)$, $a, b > 0$, $\Gamma_U = \{0\} \times (0, b)$, $\Gamma_C = (0, a) \times \{0\}$. *Then the set* $K_1 \cap C^\infty(\overline{\Omega})$ *is dense in* K_1 *with respect to the* $H^1(\Omega)$*-norm.*

P r o o f. We use the classical regularization technique. Let $\{B_j\}_{j=0}^r$ be a covering of $\overline{\Omega}$ such that

- $\overline{B}_0 \subset \overline{\Omega}$;
- B_j, $j = 1, \ldots, r$ are circles with centers on $\partial\Omega$ and radius less or equal to $\min(a/2, b/2)$.

In addition, we will suppose that four of these circles, say $B_1, \ldots, B_4$ have their centers at the corners of Ω and the remaining ones have a positive distance from the corners. Let $\{\varphi_i\}_{i=0}^r$ be the respective partition of unity, i.e. $\varphi_i \in C_0^\infty(B_i)$, $0 \leqslant \varphi_i \leqslant 1 \ \forall\, i = 0, \ldots, r$, $\sum\limits_{i=0}^r \varphi_i(x) = 1 \ \forall x \in \overline{\Omega}$, and let us denote $u_j := u\varphi_j$.

Let B_1 be the circle with the center at $A_1 = (0, 0)$. Next we show how to approximate u_1. From the definition of u_1 we see that $u_1 \in H^1(B_1 \cap \Omega)$ and $u_1 \geqslant 0$ on $\partial(\operatorname{supp} u_1)$ (see Fig. 3.5).

One can construct a non-negative prolongation of the trace u_1 from $\partial(\operatorname{supp} u_1)$ to $\operatorname{supp} u_1$, i.e. there exists a function $z_1 \in H^1(\operatorname{supp} u_1)$ such that

$$\begin{aligned} z_1 &\geqslant 0 \quad \text{in } \operatorname{supp} u_1, \\ z_1 &= u_1 \quad \text{on } \partial(\operatorname{supp} u_1). \end{aligned}$$

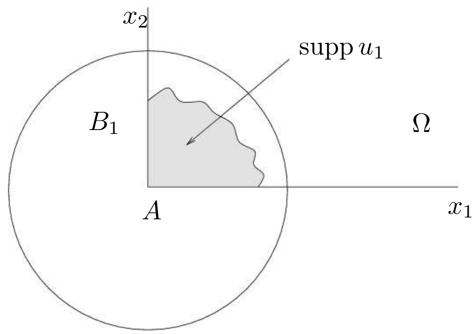

Figure 3.5.

The function z_1 can be extended by zero from $\operatorname{supp} u_1$ to $B_1 \cap \Omega$. The extended function will be denoted again by z_1. Next, u_1 will be split and written as the sum

$$u_1 = z_1 + w_1,$$

where $w_1 \in H^1(B_1 \cap \Omega)$ is such that $w_1 = 0$ on $\partial(\operatorname{supp} u_1)$. Using the classical density result we know that there exists a sequence $\{w_1^\kappa\}$, $\kappa \to 0+$ such that

(3.9) $\quad w_1^\kappa \in C^\infty(\overline{B}_1 \cap \overline{\Omega}) \quad \forall\, \kappa > 0;$

(3.10) $\quad w_1^\kappa$ vanishes in some $\delta := \delta(\kappa) > 0$ neighbourhood of $\operatorname{supp} u_1 \ \forall\, \kappa > 0;$

(3.11) $\quad w_1^\kappa \to w_1$ as $\kappa \to 0+$ in $H^1(B_1 \cap \Omega)$.

Denote by $R_1 z_1$ the even extension of z_1 with respect to the x_1-axis. Then $R_1 z_1 \in H_0^1(B_1^+)$, where $B_1^+ = \{x = (x_1, x_2) \in B_1,\ x_1 \geqslant 0\}$ and $R_1 z_1 \geqslant 0$ in B_1^+. Then one can construct a sequence $\{z_1^\kappa\}$, $\kappa \to 0+$ such that

(3.12) $$z_1^\kappa \in C_0^\infty(B_1^+) \quad \forall\, \kappa > 0;$$

(3.13) $$z_1^\kappa \to R_1 z_1, \quad \kappa \to 0+ \ \text{ in } H^1(B_1^+);$$

(3.14) $$z_1^\kappa \geqslant 0 \quad \text{in } B_1^+.$$

Let us set $u_1^\kappa := w_1^\kappa + z_1^\kappa|_{B_1 \cap \Omega}$. Then $u_1^\kappa \in C^\infty(B_1 \cap \Omega)$ for every $\kappa > 0$ and

(3.15) $$u_1^\kappa \to u_1, \quad \kappa \to 0+ \ \text{ in } H^1(B_1 \cap \Omega),$$

by virtue of (3.11) and (3.13). Finally, in view of (3.10), (3.12) and (3.14) every u_1^κ vanishes in a neighbourhood of $\Gamma_U \cap B_1$ and is non-negative in a vicinity of $\Gamma_C \cap B_1$. The remaining functions u_j, $j = 2, \ldots, r$ can be approximated in a similar way. $\square$

From Lemma 3.1 the density of $K \cap (C^\infty(\overline{\Omega}))^2$ in K readily follows. The assumption (2.6) is now an easy consequence of the previous density result. Indeed, let $v \in K$ and $\eta > 0$ be given. Then there exists a function $\overline{v} \in K \cap (C^\infty(\overline{\Omega}))^2$ such that

$$\|v - \overline{v}\|_{1,\Omega} \leqslant \eta/2. \tag{3.16}$$

The function $\overline{v}$ can be approximated by its piecewise linear Lagrange interpolant $r_h\overline{v}$ over $\mathcal{D}_h$ which belongs to K_h:

$$\|\overline{v} - r_h\overline{v}\|_{1,\Omega} \leqslant \eta/2 \quad \forall\, h \leqslant h_0(\overline{v}, \eta). \tag{3.17}$$

From (3.16), (3.17) and the triangle inequality we arrive at (2.6).

Since all assumptions of Theorem 2.1 are satisfied, there exists a subsequence $\{(u_{h'}, \Xi_{h'})\}$ of solutions to (3.8) such that

$$\begin{cases} u_{h'} \to u & \text{in } (H^1(\Omega))^2; \\ \Xi_{h'} \rightharpoonup \Xi & \text{in } L^2(\Gamma_C),\ \ h' \to 0+\,. \end{cases}$$

We now shortly describe the numerical realization of (3.8). Since the bilinear form a is symmetric we first construct the discrete superpotential $\mathcal{L}$ which is the sum of a quadratic part and a Lipschitz continuous perturbation Ψ defined by (2.10). Let Φ be a primitive function to b:

$$\Phi(x) = \int_0^x b(t)\,\mathrm{d}t.$$

Then

$$\Psi(\boldsymbol{v}) = \sum_i c_i \Phi((\boldsymbol{\Lambda v})_i)$$

where $c_1 = 3/2h$, $c_2 = \ldots = c_{m-1} = h$, $c_m = h/2$ and $(\boldsymbol{\Lambda v})_i :=$ the x_2-component of the nodal displacement vector $\boldsymbol{v}$ at x_h^i, $i = 1, \ldots, m$, the definition of P_h and Π being taken into account.

Instead of the algebraic hemivariational inequality $(\vec{\mathcal{P}})$ resulting from (3.8) we shall solve the substationary type problem $(\vec{\mathcal{P}})'$ for the superpotential $\mathcal{L}$ on $\mathcal{K}$. Since the mapping P_h satisfies (2.9), the two problems $(\vec{\mathcal{P}})$ and $(\vec{\mathcal{P}})'$ are equivalent in the sense of Theorem 2.2 provided that the one-sided limits $b(\xi\pm)$ exist for every $\xi \in \mathbb{R}$. Problem $(\vec{\mathcal{P}})'$ will be solved by a nonsmooth variant of the Newton method introduced and analyzed in [5]. We obtain an approximation of the displacement vector $\boldsymbol{u}$. From the knowledge of $\boldsymbol{u}$ one can compute the respective $\boldsymbol{\Xi}$ using the procedure described in [4, pp. 147–149]. In this way one can easily check whether the computed solution $\boldsymbol{u}$ is good enough or not.

In the rest of this section we give the formulation of a contact problem with the classical Signorini conditions and nonmonotone friction. The domain Ω and the decomposition of $\partial\Omega$ into Γ_U, Γ_P and Γ_C is the same as before. On Γ_U the body is fixed, while along Γ_C it is supported by a rigid foundation. The following unilateral (non-penetration) and friction conditions are prescribed on Γ_C:

$$u_2 \geqslant 0, \;\; T_2 \geqslant 0, \;\; u_2 T_2 = 0 \;\text{ a.e on }\; \Gamma_C; \tag{3.18}$$

$$-T_1(x) \in \hat{b}(u_1(x)) \;\text{ a.e. on }\; \Gamma_C. \tag{3.19}$$

The multifunction $\hat{b}$ again results from a function b satisfying (2.1) and (2.2) with $q = q' = 2$. Typical examples of b will be shown in the next section (see Fig. 4.6). The body is subject to surface tractions $P \in (L^2(\Gamma_P))^2$ acting on Γ_P (the volume forces are again absent). The *weak formulation* of our problem reads as follows:

$$\begin{cases} \text{Find } \; (u, \Xi) \in K \times L^2(\Gamma_C) \; \text{ such that} \\ a(u, v-u) + \int_{\Gamma_C} \Xi(v_1 - u_1)\,\mathrm{d}x_1 \geqslant \int_{\Gamma_P} P \cdot (v-u)\,\mathrm{d}s \quad \forall\, v \in K \\ \Xi(x) \in \hat{b}(u_1(x)) \; \text{ a.e on } \; \Gamma_C, \end{cases} \tag{3.20}$$

where the convex set K and the bilinear form a are the same as before. It is easy to see that $\Xi = -T_1$ on Γ_C.

One can prove again the existence of at least one solution to (3.20). Also the approximation and the convergence analysis can be done in the same way as in the previous example.

4. Model examples

In this section numerical results of several simple delamination and nonmonotone friction problems will be presented. Geometrical and material characteristics are the same in all these examples, namely $\Omega = (0, 100) \times (0, 10)$ (in mm), $E = 2.1 \times 10^5\,\mathrm{N/mm^2}$, $\sigma = 0.3$, $t = 5\,\mathrm{mm}$.

The domain Ω is carved into small squares of size h and each square is divided into two triangles in a way depicted in Fig. 4.1. The system of all triangles creates the triangulation $\mathcal{D}_h$. In our computations we have used the following grids: 20×2, 40×4, 60×6, 80×8.

We start with a delamination problem. Let us suppose that P defining the surface traction T is *a positive constant* on $(50, 100) \times \{10\}$. The multifunction $\hat{b}$ in (3.2) is represented by piecewise linear segments determined by the nodes (see Fig. 3.2) $A = (0.1, 0.5)$, $B = (0.1, 0.3125)$, $C = (0.2, 0.4375)$, $D = (0.2, 0.1875)$, $E = (0.3, 0.3125)$, $F = (0.3, 0.125)$, $G = (0.4, 0.1875)$, $H = (0.4, 0)$.

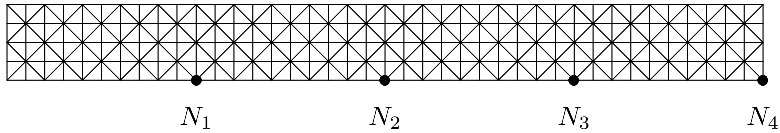

Figure 4.1.

To reduce the total number of unknowns in the substationary problem $(\vec{\mathcal{P}})'$, we use the *condensation* technique, i.e. all variables except those corresponding to the vertical displacements on Γ_C will be eliminated. The resulting (HI) contains considerably less unknowns than the original one. As we have already mentioned, problem $(\vec{\mathcal{P}})'$ was solved by a nonsmooth variant of the Newton method. This method is based on a piecewise quadratic approximation of minimized functions. The most important parameters for tuning the subroutine are chosen as follows (for their detailed description see [6]):

distance measure parameter `ETA` $= 0.01$, distance measure exponent `MOS` $= 1$, maximum stepsize `XMAX` $= 10^{-6}$, maximum bundle dimension $= 43$.

The computed values of the horizontal and vertical displacements at the particular points N_1, N_2, N_3, N_4 on Γ_C for the grid 40×4 and for different values of P are shown in Tables 1 and 2.

P [N/mm^2]	$u_1(N_1)$	$u_1(N_2)$	$u_1(N_3)$	$u_1(N_4)$
0.1	0.001917	0.003070	0.003517	0.003580
0.2	0.003846	0.006161	0.007060	0.007187
0.3	0.005780	0.009260	0.010610	0.010800
0.4	0.007714	0.012357	0.014160	0.014413
0.5	0.009649	0.015456	0.017711	0.018028

Table 1. The horizontal displacements in mm.

P [N/mm^2]	$u_2(N_1)$	$u_2(N_2)$	$u_2(N_3)$	$u_2(N_4)$
0.1	0.005271	0.018197	0.035015	0.052887
0.2	0.010577	0.036519	0.070275	0.106148
0.3	0.015896	0.054883	0.105613	0.159526
0.4	0.021214	0.073242	0.140942	0.212889
0.5	0.026535	0.091611	0.176288	0.266279

Table 2. The vertical displacements in mm.

The horizontal and vertical displacements at the same points for different partitions of Ω are shown in Tabs. 3 and 4.

grid	$u_1(N_1)$	$u_1(N_2)$	$u_1(N_3)$	$u_1(N_4)$
20×2	0.001378	0.002209	0.002531	0.002578
40×4	0.001917	0.003070	0.003517	0.003580
60×6	0.002071	0.003317	0.003799	0.003867
80×8	0.002131	0.003411	0.003908	0.003977

Table 3. The horizontal displacements in mm ($P = 0.1\,\mathrm{N/mm^2}$).

grid	$u_2(N_1)$	$u_2(N_2)$	$u_2(N_3)$	$u_2(N_4)$
20×2	0.003857	0.013152	0.025299	0.038175
40×4	0.005271	0.018197	0.035015	0.052887
60×6	0.005705	0.019649	0.037807	0.057105
80×8	0.005862	0.020210	0.038882	0.058731

Table 4. The vertical displacements in mm ($P = 0.1\,\mathrm{N/mm^2}$).

The total deformation of the structure for $P = 0.1$ and $0.5\,\mathrm{N/mm^2}$ (enlarged $50\times$) is depicted in Figs. 4.2 and 4.3. Fig. 4.4 illustrates the distribution of the normal stresses along the contact part Γ_C. In this way, one can verify whether the computed stresses follow the diagram given by Fig. 3.2.

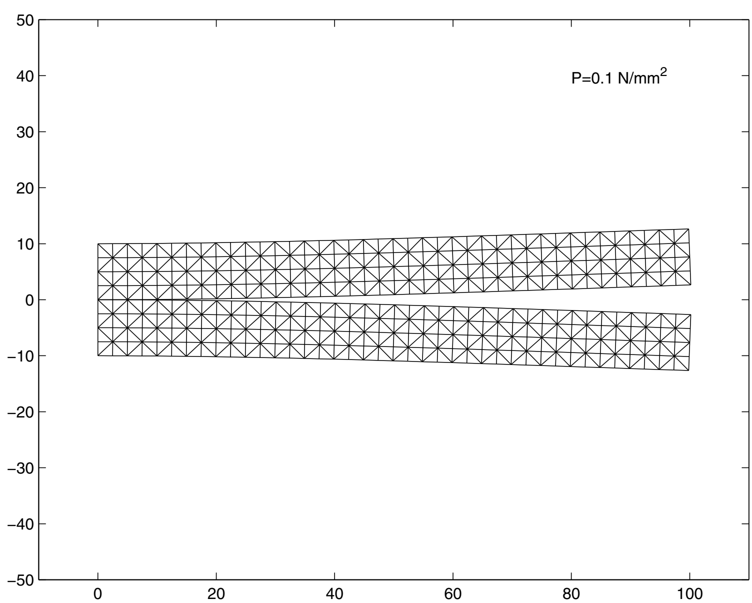

Figure 4.2.

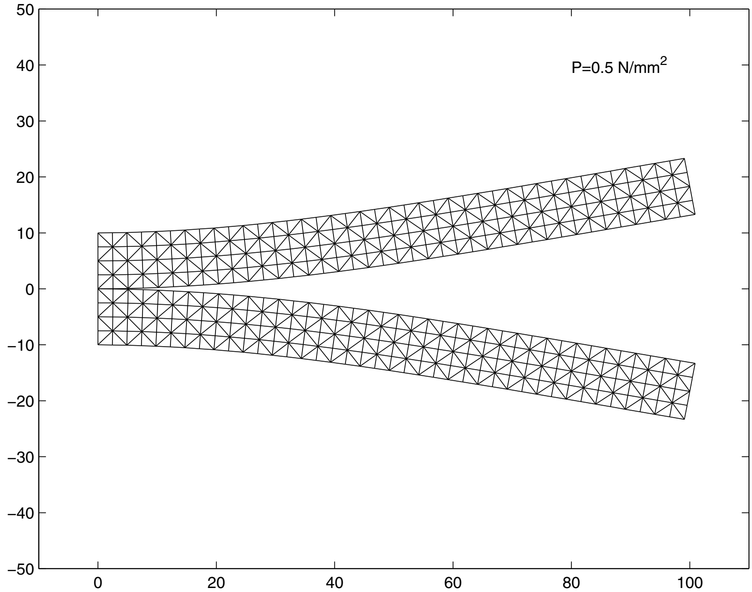

Figure 4.3.

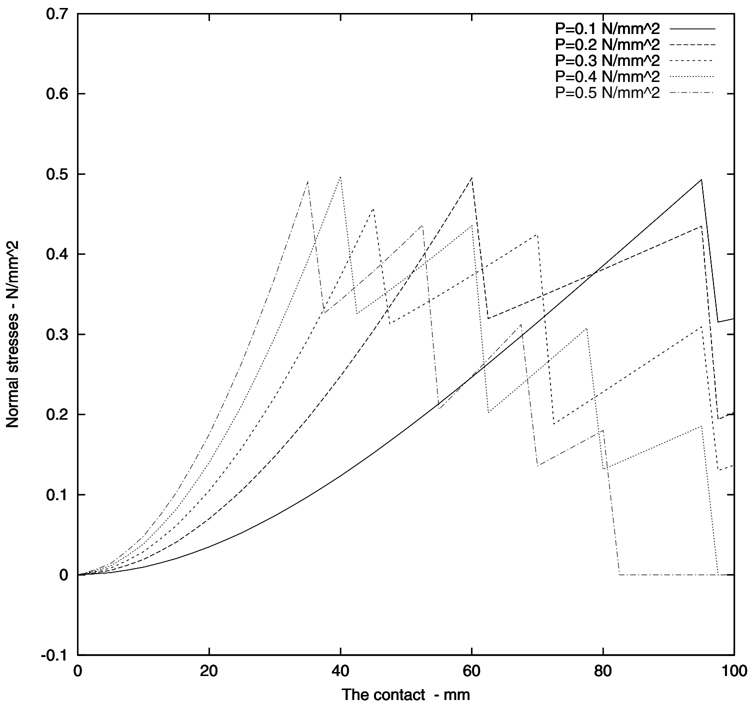

Figure 4.4. The distribution of normal stresses along Γ_C.

We close this section with numerical results of a simple Signorini problem with nonmonotone friction, whose weak formulation is given by (3.20). The body Ω is fixed along Γ_U and the surface tractions $T = (P_1, 0)$, $T = (0, P_2)$ act on $\{100\} \times [0, 10]$, $[50, 100] \times \{10\}$, respectively, where $P_1 = 0.05\,\mathrm{N/mm}^2$ and $P_2 = -0.02\,\mathrm{N/mm}^2$ (see Fig. 4.5). We shall consider two nonmonotone friction laws represented by Fig. 4.6 a), c). The obtained results will be compared with a classical monotone friction law (Fig. 4.6 b)). In our computations the 40×4 grid was used (see Fig 4.1). The graph of the tangential component of the displacement and the stress vector along Γ_C are shown in Figs. 4.7 and 4.8, respectively. Figs. 4.9 and 4.10 show the graphs of the normal components of the displacement and the stress vector, respectively, along Γ_C. Finally, the total deformation of Ω enlarged $10^6\times$ is depicted in Fig. 4.11.

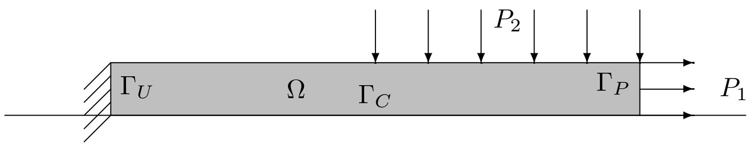

Figure 4.5.

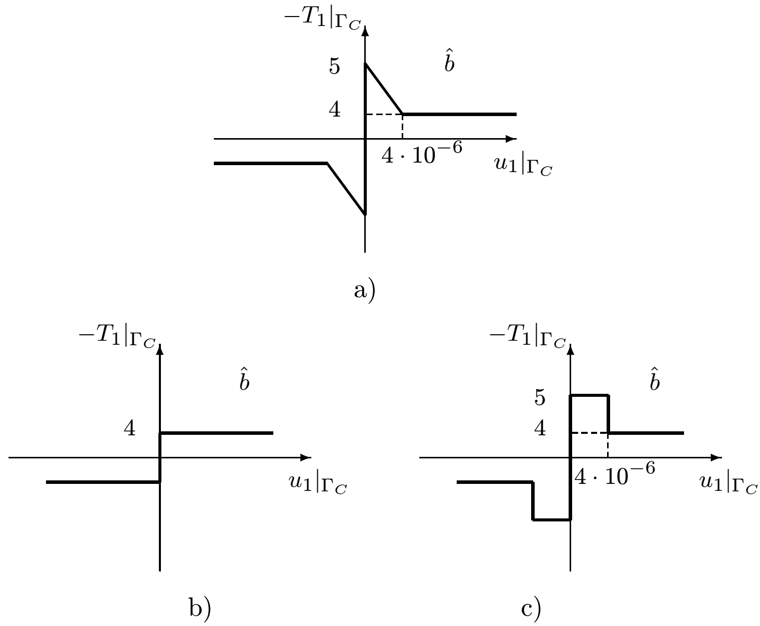

Figure 4.6.

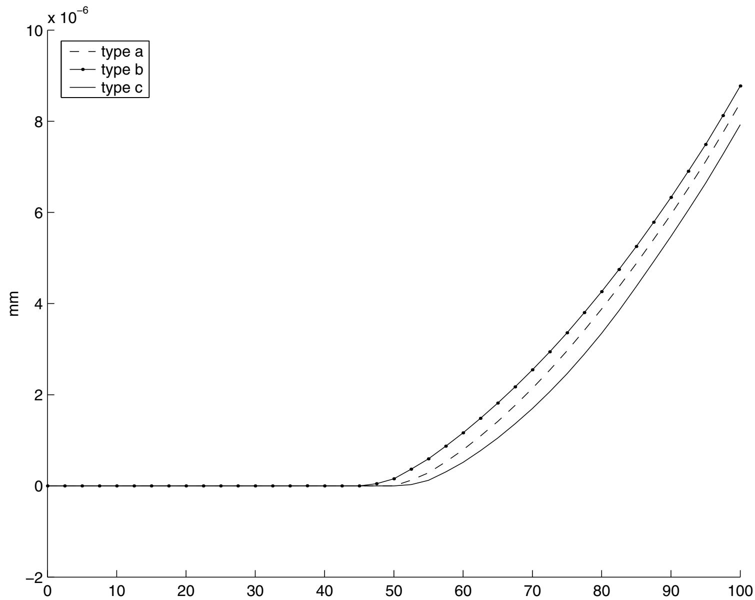

Figure 4.7. The tangential component of the displacement vector on Γ_C.

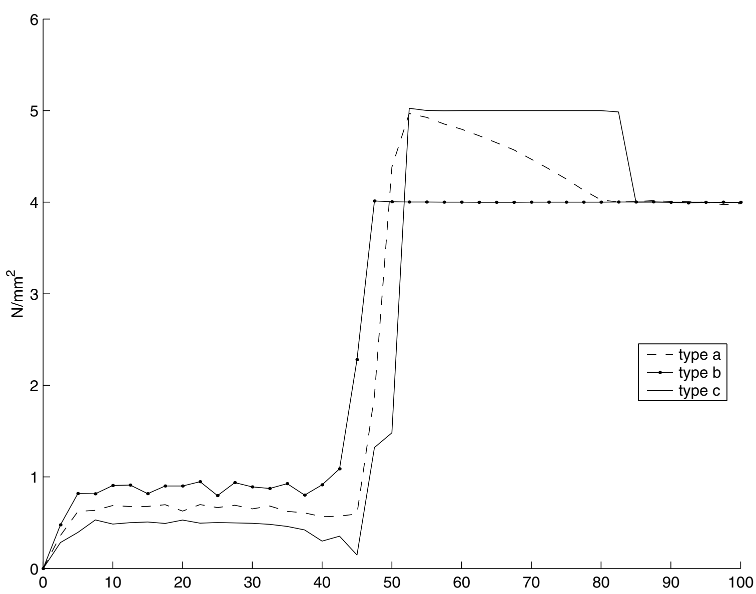

Figure 4.8. The tangential component of the stress vector on Γ_C.

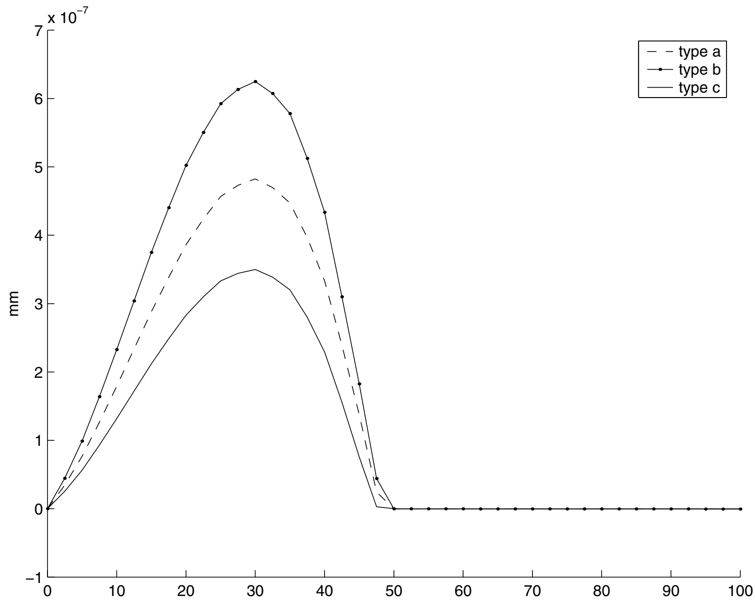

Figure 4.9. The normal component of the displacement vector on Γ_C.

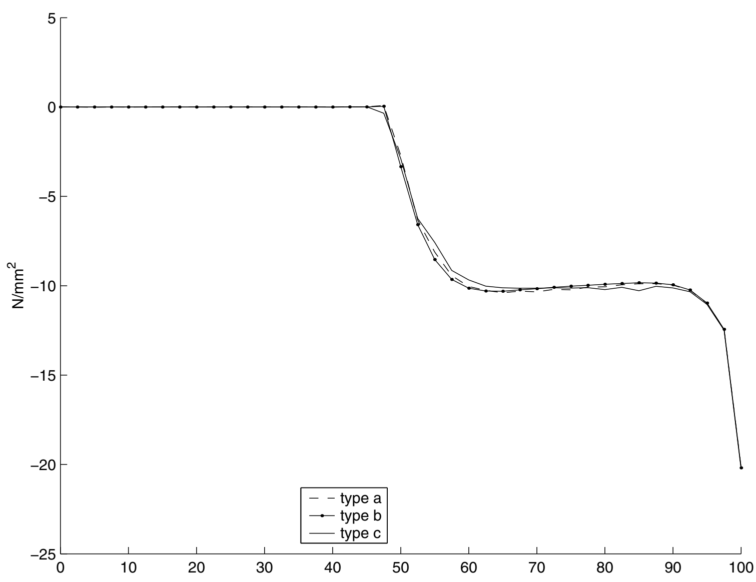

Figure 4.10. The normal component of the stress vector on Γ_C.

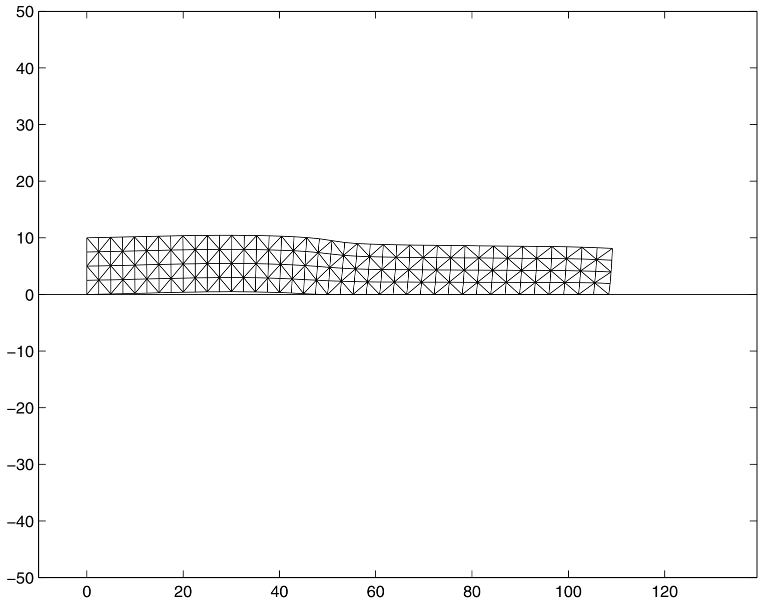

Figure 4.11.

References

[1] *K. C. Chang*: Variational methods for non-differentiable functionals and their applications for partial differential equations. J. Math. Anal. Appl. *80* (1981), 102–129.

[2] *R. Glowinski, J.-L. Lions, R. Trémolières*: Numerical Analysis of Variational Inequalities. Studies in Mathematics and its Applications, Vol. 8. North Holland, Amsterdam, New York, 1981.

[3] *A. K. Green, W. H. Bowyer*: The testing and analysis of novel top-hat stiffener fabrication methods for use in GRP ships. Proceedings from the 1st International Conference "On Composite Structures" (I. H. Marshal, ed.). Applied Science Publishers, London, 1981, pp. 182–201.

[4] *J. Haslinger, M. Miettinnen, and P. D. Panagiotopoulos*: Finite Element Method for Hemivariational Inequalities. Theory Methods and Applications 35. Kluwer Academic Publishers, Dordrecht, 1999.

[5] *L. Lukšan, J. Vlček*: A bundle-Newton method for nonsmooth unconstrained minimization. Math. Program. *83 A* (1998), 373–391.

[6] *L. Lukšan, J. Vlček*: PBUN, PNEW—a bundle type algorithms for nonsmooth optimization. Technical Report No. V-718, Sept. 1997.

[7] Topics in Nonsmooth Mechanics (J. J. Moreau, P. D. Panagiotopoulos, and G. Strang, eds.). Birkhäuser-Verlag, Basel, 1988.

[8] *E. Moyson, D. van Gemert*: Experimentelle Prüfungen der Laminat-Theorie für Faserverstärkte Verbundwerkstoffe. Proceedings Verbundwerkstoffe, Phasenverbindung und Mechanische Eigenschaften, Vol. I (G. Ondracek, ed.). Deutsche Gesellschaft für Metallkunde, Karlsruhe, 1985, pp. 99–115.

[9] *P. D. Panagiotopolous*: Inequality Problems in Mechanics and Applications. Convex and Nonconvex Energy Functions. Birkhäuser-Verlag, Basel-Boston-Stuttgart, 1985.

[10] *P. D. Panagiotopoulos*: Hemivariational Inequalities. Applications in Mechanics and Engineering. Springer-Verlag, Berlin, 1993.
[11] *I. Roman, H. Harlet, and G. Marom*: Stress intensity factor measurements in composite sandwich structures. In: Proceedings of the 1st International Conference on Composite Structures (I. H. Marshal, ed.). Applied Science Publishers, London, 1981, pp. 633–645.
[12] *M. M. Schwartz*: Composite Materials Handbook. McGraw Hill, New York, 1984.
[13] *N. S. Shidharan*: Elastic and strength properties of continuous chopped glass fiber hybrid sheet molding compounds. Short Fiber Reinforced Composite Materials ASTM STP, Vol. 787. Philadelphia, 1982, pp. 167–179.
[14] *J. G. Williams, M. D. Rhodes*: Effect of resin on impact damage tolerance of graphite/epoxy laminates. Proceedings of the 6th International Conference on Composite Materials, Testing and Design ASTM STP, Vol. 787. Philadelphia, 1982, pp. 450–480.

Authors' addresses: *C. C. Baniotopoulos*, Civil Engineering Department, Aristotle University, Thessaloniki, Greece, e-mail: `ccb@civil.auth.gr`; *J. Haslinger*, Charles University, Faculty of Mathematics and Physics, KNM, Sokolovská 83, CZ 186 75 Praha 8, Czech Republic, e-mail: `Jaroslav.Haslinger@mff.cuni.cz`; *Z. Morávková*, VŠB TU Ostrava, 17. listopadu 15, CZ 708 33 Ostrava-Poruba, Czech Republic, e-mail: `zuzana.moravkova@vsb.cz`.